A cutting strategy with continuously varying stepover to suppress the diffraction effect of ultra-precision machined surfaces

Yangqin Yu and Xinquan Zhang#

School of Mechanical Engineering, Shanghai Jiao Tong University, Shanghai 200240, China
Corresponding Author / Email: zhangxinquan@sjtu.edu.cn

KEYWORDS: Ultra-precision machining, Diffraction effect, Periodic surface texture, Continuously varying stepover

Diffraction effect has been troubling optical elements fabricated by ultra-precision machining for decades, which results in energy loss and imaging quality degradation. Such effect is assumed to result from the periodic micro textures similar to diffraction gratings which are generated during machining. To provide a possible solution, a continuously varying stepover cutting method is designed in this study to disrupt the periodic tool marks during slow tool servo turning. Tiny harmonic variations are integrated into the spiral cutting motion. The influence of amplitude and period of the variation on the resultant surface topography is investigated. A theoretical model is established to predict the periodic micro textures fabricated by the proposed method. Machining experiments with various magnitudes and periods are designed and conducted. Both measured topography and power spectral density analysis demonstrates disrupted textures with multiple frequencies. Suppressed diffraction effect is observed on machined surface. It is indicated by the results that variation with relatively small amplitude is conducive to suppressing the diffraction effect of ultra-precision machined optical elements while maintaining surface finish.

1. Introduction

Ultra-precision machining has been widely adopted as a nanoscale fabrication technology by both the industry and the academia. However, optical surfaces fabricated by ultra-precision machining inevitably suffer from diffraction effect, which has demonstrated harmful to desired optical performance and function [1]. Extensive research on postprocessing techniques [2] like polishing and lapping has provided means to eliminate the diffraction effect, but the total cost and time would be significantly increased. Therefore, great effort are being made to investigate the cause and suppression methods of diffraction effect by ultra-precision machining.

It is indicated by existing research that one major cause of the diffraction effect is the periodic micro textures [3] on machined surfaces. The constant stepover of tool path driving spiral make them similar to optical gratings [4] which require a precise control of the period as shown in Fig. 1. Wu et al. [5] found that residual cutting marks cause serious diffraction and optical performance deterioration of the machined surface. Cheung and Lee [6] conducted multi-spectrum analysis on diamond turned surfaces and identified a single predominant frequency component with the spatial period identical to machining stepover. Stover [7] classified diamond turned surfaces into two-dimensional random, periodic tool mark structured and one-dimensional random surfaces and investigated corresponding resultant diffraction effects. In conclusion, the diffraction effect of ultra-precision machined surfaces is majorly caused by the periodic micro textures generated during machining with constant stepover.

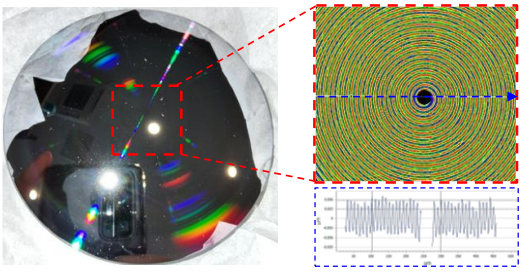

Fig. 1 Ultra-precision turned surface suffering from diffraction effect

In recent years, attempts on suppressing the diffraction effect by novel machining methods have been made. Wang et al. [8] acquired the critical stepover for turned surfaces to show diffraction effect utilizing a blazed grating theoretical model. Weng et al. [9] monitored the turning process by acoustic emission and identified the correlation between the high-frequency energy of AE signal and the diffraction effect. Zhu [10] developed a Pseudo-random Diamond Turning method utilizing fast tool servo for the suppression of scattering effects. The pseudo-random spatial spiral cutting motion with random stepover proved effective in generating partly random micro textures. He et al. [11] developed an accurate surface topography model which integrated tool edge waviness, spindle vibration and material mechanical behaviors to guide the machining process. Diamond tool with deteriorated waviness [12] was found to enhance the diffraction effect and a waviness controlled tool is recommended.

Since the periodic micro textures are generated by the spiral machining motion, tool path modification is a direct and reasonable approach to disrupt the periodic micro textures without additional postprocessing. Current relevant research focuses on the suppression

of the diffraction effect without considering the negative influence of tool path modification on the surface finish.

In this study, a cutting strategy with continuously varying stepover is proposed to disrupt the periodic micro textures without inducing major surface finish degradation. Instead of using totally random stepover that harms surface finish, the proposed method realizes continuously varying stepover. Abrupt high-frequency vibrations can be avoided. The method to realize continuously varying stepover is established by incorporating harmonic variations. A theoretical model for three-dimensional surface topography prediction is elaborated. Disrupted surface topography is successfully acquired, and diffraction effect is suppressed as demonstrated by experimental results.

2. Generation of tool path with continuously varying stepover and surface topography simulation

2.1 Models for periodic micro textures

The theoretical models for the periodic micro textures after turning on planar, concave and convex surfaces are established as illustrated in Fig. 2. The diamond tool cutting edge is approximated as a prefect spherical curve.

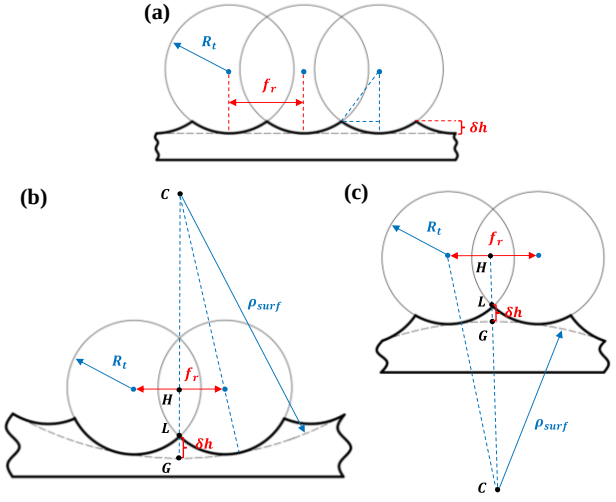

Fig. 2 Models for periodic micro textures of machined surface: (a) for planar surface, (b) for concave surface, and (c) for convex surface

For a planar surface, the peak residual height δh can be simply calculated by tool nose radius R_t and stepover f_r as:

$$\delta h = R_t - \sqrt{{R_t}^2 - (f_r/2)^2} \tag{1}$$

For a concave or a convex surface, δh can be expressed as:

$$\delta h = CG - CH - HL, \text{ for concave surface} \tag{2}$$

$$\delta h = CH - CG - HL, \text{ for concave surface} \tag{3}$$

Solve each line segment with tool nose radius R_t, stepover f_r and base surface spherical radius ρ_{base}, then equations can be rewritten as:

$$\delta h_{CC} = \rho_{surf} - \sqrt{\left(\rho_{surf} - R_t\right)^2 - \left(\frac{f_r}{2}\right)^2} - \sqrt{{R_t}^2 - \left(\frac{f_r}{2}\right)^2} \tag{4}$$

$$\delta h_{CV} = \sqrt{\left(\rho_{surf} + R_t\right)^2 - \left(\frac{f_r}{2}\right)^2} - \rho_{surf} - \sqrt{{R_t}^2 - \left(\frac{f_r}{2}\right)^2} \tag{5}$$

Eq. 4 and 5 are for concave and convex surfaces respectively.

With the peak residual height δh acquired, the residual height distribution near the peak can be obtained using the tool edge curve.

2.2 Realization of continuously varying stepover

As already demonstrated in Fig. 1 and Fig. 2, conventional turning tool path driven by Archimedean spirals result in inevitable periodic surface micro textures, which is assumed to cause diffraction effect. Therefore, the method to realize driving spirals with continuously varying stepover is developed by integrating tiny harmonic variations along the feed direction, as depicted in Fig. 3.

The standard planar Archimedean driving spiral for turning can be expressed in the polar coordinate system as:

$$\rho(\theta) = \rho_0 - \frac{f_r \theta}{2\pi} \tag{6}$$

where ρ_0 means the outermost radius and f_r represents the stepover of the driving spiral. And a point on the spiral is expressed as (ρ, θ).

If equal angle interval discretization with N points in each revolution is adopted, then the n-th point on the m-th revolution can be written as:

$$\begin{cases} \theta_{m,n} = 2\pi(m + n/N) \\ \rho_{m,n} = \rho_0 - f_r(m - 1 + n/N) \end{cases} \tag{7}$$

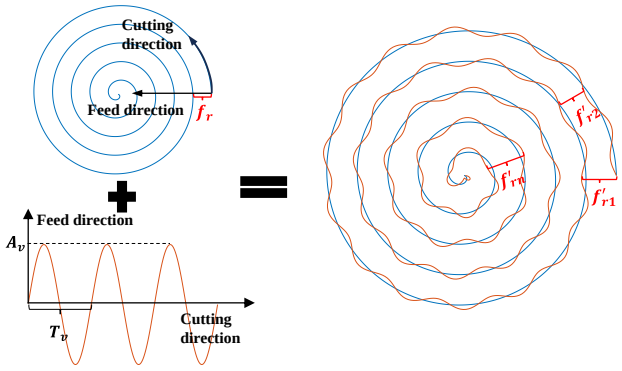

Fig. 3 Realization of driving spiral with continuously varying stepover

Now incorporate harmonic variations into standard planar Archimedean driving spiral. Represent the modified spiral as:

$$\rho'(\theta) = \rho_0 - \frac{f_r \theta}{2\pi} + \Delta\rho_v \tag{8}$$

where θ remains the same as in (6), and $\Delta\rho_v$ stands for the component of radial variations with amplitude A_v and period T_v.

$$\Delta\rho_v(\theta) = A_v \sin\left(2\pi \frac{\theta}{T_v}\right) \tag{9}$$

The harmonic variations can be designed to have various amplitudes $A_{v,i}$ and periods $A_{v,i}$ in each segment, in which case $\Delta\rho_{v,i}$ is expressed as:

$$\begin{cases} \Delta\rho_{v,i}(\theta) = A_{v,i} \sin\left(2\pi \frac{\theta - \theta_0}{T_{v,i}}\right) \\ \theta_0 = \sum_{k=1}^{i-1} T_{v,k} \end{cases} \tag{10}$$

As illustrated in Fig. 3, continuously varying stepover is realized in the modified driving spiral, which is expected to disrupt the periodic surface micro textures of turned surfaces.

2.3 Simulation of 3D surface topography

Based on the surface texture model in section 2.1 and the irregular driving spiral in section 2.2, this study further established a simulation method for predicting the 3D surface topography when utilizing a continuously varying stepover.

Firstly, the 2D grid for surface topography calculation is defined. For example, a polar grid $\{P_{j,k}(\rho_j, \theta_k, z_{j,k})\}$ is established in Fig. 4 (a).

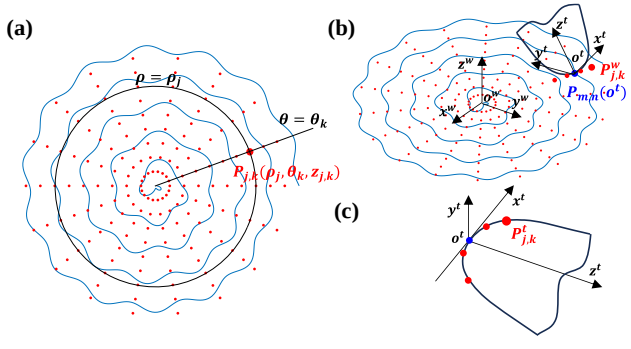

Fig. 4 Surface topography simulation: (a) definition of the polar grid, (b) identification of points near a CLP in the workpiece coordinate system, and (c) calculation of Z values in the tool coordinate system

Next, calculate the $z_{j,k}$ values of the grid by moving the diamond tool along the driving spiral and replicate the tool curve onto the grid surface. Assume the cutter location point (CLP) is $P^w_{m,n}(\rho_{m,n}, \theta_{m,n}, z_{m,n})$ for this moment, which coincides with the origin o^t of the tool coordinate system, as shown in Fig. 4 (b). Grid points $\{P^w_{j,k}\}$ in the workpiece coordinate system near $P_{m,n}$ can be determined by:

$$\{P^w_{j,k}(\rho_j, \theta_k, z_{j,k}) \mid \theta_k = \theta_{m,n}, \mathrm{abs}(\rho_j - \rho_{m,n}) \le \xi_\rho\} \quad (11)$$

where ξ_ρ is a manually set value typically smaller than f_r.

Then, find their corresponding points $\{P^t_{j,k}(x^t_{j,k}, y^t_{j,k}, z^t_{j,k})\}$ in the tool coordinate system through coordinate transformation, as shown in Fig. 4 (c):

$$\begin{pmatrix} \boldsymbol{P^t_{j,k}} \\ \mathbf{1} \end{pmatrix} = \begin{pmatrix} \cos(-\theta_k) & -\sin(-\theta_k) & 0 & -\rho_j \\ \sin(-\theta_k) & \cos(-\theta_k) & 0 & 0 \\ 0 & 0 & 1 & 0 \\ 0 & 0 & 0 & 1 \end{pmatrix} \begin{pmatrix} \boldsymbol{P^w_{j,k}} \\ \mathbf{1} \end{pmatrix} \quad (12)$$

Now that the $x^t_{j,k}$ and $y^t_{j,k}$ of $\{P^t_{j,k}\}$ are acquired, the Z values $z^t_{j,k}$ can be obtained utilizing the tool curve function f^t_{tool}:

$$z^t_{j,k} = f^t_{tool}(x^t_{j,k}, y^t_{j,k}) \quad (13)$$

The $z^w_{j,k}$ value of surface topography at $P^w_{j,k}$ can be determined:

$$z^w_{j,k} = z^t_{j,k} + z^w_{m,n} \quad (14)$$

To be noted, if multiple $z^w_{j,k}$ values are acquired for the same grid point, then the minimum one is kept as the outcome.

Using the simulation method described above, typical surface topographies are acquired as illustrated in Fig. 5. For driving spirals with constant stepover, the surface topography is completely regular and periodic micro textures similar to optical gratings can be clearly identified along the feed direction. For (b) and (c) with continuously varying stepovers, the periodic textures are successfully disrupted and the original stepover is no longer predominant. Moreover, slightly varying stepover, where the variations are smaller than f_r, generates relatively smaller surface residual height than severely varying stepover. The surface finish generated by slightly varying stepover is also expected to be much better than the latter.

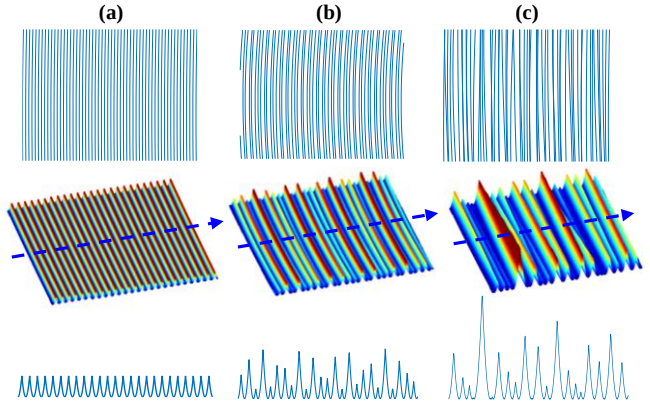

Fig. 5 Typical surface topography acquired by simulation: (a) constant stepover, (b) slightly varying stepover, and (c) severely varying stepover

3. Experiments and results

3.1 Experimental setup

Turning experiments with varying stepovers are designed and conducted to validate the proposed cutting strategy. A commercial Moore Nanotech 250FG ultra-precision machine tool as shown in Fig. 6 is utilized to perform the experiments.

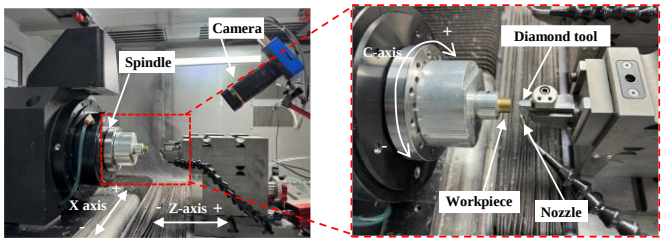

Fig. 6 Experimental setup

Six tests are conducted on a planar brass workpiece under the slow tool servo (STS) mode. Detailed parameters for the tests are listed in Table. 1. A diamond tool with radius R_T of 1 mm is used and the original stepover f_r is set as 10 μm. The amplitude A_v and period T_v of the introduced harmonic variations as depicted in Fig. 3 are designed to be different for each group for comparative analysis. Test 1 adopts a constant stepover of 10 μm for comparison. For tests 2 to 5, an amplitude of 2 μm is employed to generate slightly varying stepover while an amplitude of 10 μm for severely varying stepover. And the amplitude and period of test 6 are designed to be random.

Table. 1 Test design and harmonic variation parameters

Test No.	1	2	3	4	5	6
Amplitude, A_v (μm)	0	2	10	2	10	2-10
Period, T_v (Points)	—	157	157	397	397	157-397

3.2 Experimental results

Surface topography of machined surface is measured with a white light interferometer (Zygo Nexview NX2) and the results are shown in Fig. 7.

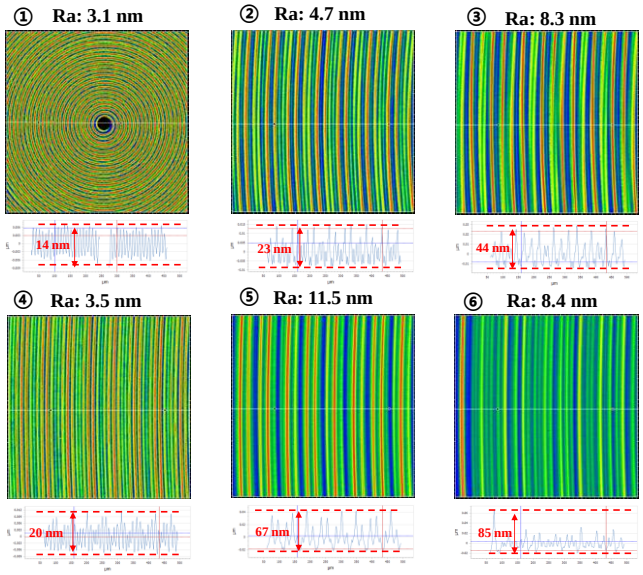

Fig. 7 Surface topography measurement results

The measured topography coincide well with the simulation results in Fig. 5. For test 1, periodic micro textures similar to optical gratings can be clearly distinguished in both the 3D topography and the cross-section plot, which are assumed to cause the diffraction of turned surfaces. But it generates the best surface finish with a roughness Ra of 3.1 nm and the lowest residual height of 14 nm among all 6 tests. For tests 2 to 6, disrupted surface textures with multi-level structures are observed instead of a single structure. Test 6 with random variation and tests 3 and 5 with severely varying stepover generate more irregular surfaces with more than twice the roughness of test 1. In comparison,

tests 2 and 4 generate surfaces with roughness approximating test 1 while realizing disrupted surface textures at the same time.

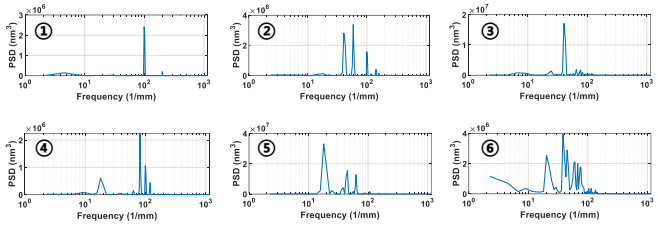

Fig. 8 Power spectral density (PSD) analysis results

Power spectral density (PSD) analysis is conducted for the measured topographies as shown in Fig. 8. Cross-sections along the feed direction of Fig. 7 are transformed into the spatial frequency region to distinguish components with various frequencies. The PSD plot of test 1 demonstrates typical single-peak spatial frequency distribution at 100 mm^{-1}, which corresponds to the periodic textures with period of 10 μm f_r. For tests 2 to 6, multiple frequency components are incorporated and the peak at 100 mm^{-1} is no longer dominant. Such scattered frequency distribution is conducive to suppressing the diffraction effect caused by mono-frequency surface textures. Theoretically, the more scattered the frequency distribution is, the less diffraction effect takes place.

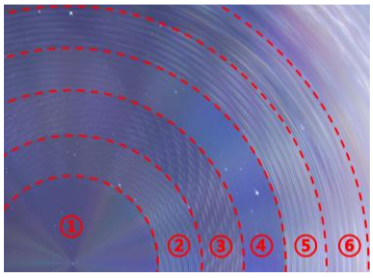

Fig. 9 Optical inspection result

Optical inspection result is acquired as Fig. 9 to assess the diffraction effect of 6 tests. Area of test 1, which employs constant stepover, suffer from severe diffraction effect. In comparison, area of tests 2 and 4, which employs slightly varying stepover, have significantly suppressed diffraction effect owing to the disrupted textures as represented in Fig. 8. And roughly equal surface finish to test 1 is realized. For the rest, suppressed diffraction effect is also observed, but major surface finish deteriorations happen due to the severely varying surface topography.

4. Conclusions

This study proposes a continuously varying stepover machining strategy by incorporating harmonic variations into conventional Archimedean driving spirals. Experimental investigations demonstrate that the periodic surface micro textures that cause diffraction effect are effectively disrupted by the proposed method. Major conclusions are drawn as follows:

1) Tool path driven by constant stepover spiral results in periodic surface micro textures, which are similar to optical gratings and assumed to cause the diffraction effect of turned surfaces.
2) The continuously varying stepover strategy proves effective in disrupting the periodic micro textures. Both measured surface topography and PSD analysis results demonstrate disrupted multi-frequency microstructures. Measured results coincides well with simulation.
3) Both disrupted periodic textures and surface roughness Ra of 3.5 nm are realized by slightly varying stepover. In comparison, severely varying stepover results in major surface finish deterioration.

ACKNOWLEDGEMENT

The authors gratefully acknowledge the financial support of the National Key R&D Program of China under Grant 2022YFB3403301, the National Natural Science Foundation of China under Grants 52075332, U22A20207 and 52335010, and the Science & Technology Commission of Shanghai Municipality under Grant 22511102105.

REFERENCES

[1] C. L. He and W. J. Zong, "Diffraction effect and its elimination method for diamond-turned optics," *Opt. Express*, vol. 27, no. 2, p. 1326, Jan. 2019, doi: 10.1364/OE.27.001326.

[2] Z. Z. Li *et al.*, "Removal of single point diamond-turning marks by abrasive jet polishing," *Appl. Opt.*, vol. 50, no. 16, p. 2458, Jun. 2011, doi: 10.1364/AO.50.002458.

[3] H. Hocheng, H. C. Tseng, M. L. Hsieh, and Y. H. Lin, "Tool wear monitoring in single-point diamond turning using laser scattering from machined workpiece," *Journal of Manufacturing Processes*, vol. 31, pp. 405–415, Jan. 2018, doi: 10.1016/j.jmapro.2017.12.007.

[4] N. Bonod and J. Neauport, "Diffraction gratings: from principles to applications in high-intensity lasers," *Advances in Optics and Photonics*, vol. 8, no. 1, pp. 156–199, 2016.

[5] D. Wu, C. Kang, F. Liang, G. Yan, and F. Fang, "Diffractive optical characteristics of nanometric surface topography generated by diamond turning," *Journal of Manufacturing Processes*, vol. 67, pp. 23–34, Jul. 2021, doi: 10.1016/j.jmapro.2021.04.012.

[6] C. F. Cheung and W. B. Lee, "A multi-spectrum analysis of surface roughness formation in ultra-precision machining," *Precision Engineering*, vol. 24, no. 1, pp. 77–87, Jan. 2000, doi: 10.1016/S0141-6359(99)00033-1.

[7] J. C. Stover, "Light scatter metrology of diamond turned optics," presented at the Optics & Photonics 2005, A. Duparr½Á, B. Singh, and Z.-H. Gu, Eds., San Diego, California, USA, Aug. 2005, p. 58780R. doi: 10.1117/12.613779.

[8] D. Wang, Y. Sui, H. Yang, and D. Li, "Adaptive spiral tool path generation for diamond turning of large aperture freeform optics," *Materials*, vol. 12, no. 5, p. 810, 2019.

[9] C.-Y. Weng, S.-C. Shiu, Y.-C. Cheng, and C.-W. Liu, "Acoustic emission monitoring of aspherical lens diffraction in single-point diamond turning process," *Int J Adv Manuf Technol*, vol. 130, no. 1–2, pp. 973–983, Jan. 2024, doi: 10.1007/s00170-023-12716-z.

[10] Z. Zhu, X. Zhou, D. Luo, and Q. Liu, "Development of pseudo-random diamond turning method for fabricating freeform optics with scattering homogenization," *Opt. Express*, vol. 21, no. 23, p. 28469, Nov. 2013, doi: 10.1364/OE.21.028469.

[11] C. L. He, W. J. Zong, C. X. Xue, and T. Sun, "An accurate 3D surface topography model for single-point diamond turning," *International Journal of Machine Tools and Manufacture*, vol. 134, pp. 42–68, Nov. 2018, doi: 10.1016/j.ijmachtools.2018.07.004.

[12] C. L. He, S. J. Wang, W. J. Zong, and S. T. Zhang, "Influence of tool edge waviness on the diffraction effect of diamond-turned optics: theoretical simulation and experimental validation," *Appl. Opt.*, vol. 58, no. 6, p. 1596, Feb. 2019, doi: 10.1364/AO.58.001596.